

ULTRA: Uncertainty-aware Label Distribution Learning for Breast Tumor Cellularity Assessment

Xiangyu Li¹, Xinjie Liang¹, Gongning Luo¹ (✉), Wei Wang¹, Kuanquan Wang¹ (✉), and Shuo Li²

¹ Harbin Institute of Technology, Harbin, China
 {luogongning,wangkq}@hit.edu.cn

² Western University, London, ON, Canada

Abstract. Neoadjuvant therapy (NAT) for breast cancer is a common treatment option in clinical practice. Tumor cellularity (TC), which represents the percentage of invasive tumors in the tumor bed, has been widely used to quantify the response of breast cancer to NAT. Therefore, automatic TC estimation is significant in clinical practice. However, existing state-of-the-art methods usually take it as a TC score regression problem, which ignores the ambiguity of TC labels caused by subjective assessment or multiple raters. In this paper, to efficiently leverage the label ambiguities, we proposed an **Uncertainty-aware Label Distribution Learning (ULTRA)** framework for automatic TC estimation. The proposed ULTRA first converted the single-value TC labels to discrete label distributions, which effectively models the ambiguity among all possible TC labels. Furthermore, the network learned TC label distributions by minimizing the Kullback-Leibler (KL) divergence between the predicted and ground-truth TC label distributions, which better supervised the model to leverage the ambiguity of TC labels. Moreover, the ULTRA mimicked the multi-rater fusion process in clinical practice with a multi-branch feature fusion module to further explore the uncertainties of TC labels. We evaluated the ULTRA on the public BreastPathQ dataset. The experimental results demonstrate that the ULTRA outperformed the regression-based methods for a large margin and achieved state-of-the-art results. The code will be available from <https://github.com/PerceptionComputingLab/ULTRA>.

Keywords: Breast cancer · Neoadjuvant therapy · Tumor cellularity · Label distribution learning · Label ambiguity.

1 Introduction

Breast cancer is one of the most common cancers for women worldwide [1]. For breast cancer treatment, neoadjuvant therapy (NAT) [2], which aims to reduce the tumor size and avoid mastectomy for patients, is a common treatment option in clinical practice [3, 4]. Tumor cellularity (TC), which represents the percentage of invasive tumors in the tumor bed, has been widely used to quantify the

response of breast cancer to NAT [5–7]. Besides, TC is also a significant indicator of the residual cancer burden (RCB), which predicts cancer recurrence and patients’ survival [8]. In the current clinical practice, TC is estimated by the pathologists on hematoxylin and eosin (H&E)-stained slides, which is rather time-consuming and suffers from inter-rater and intra-rater variability [9]. Therefore, it is highly desirable to develop automatic and reliable methods for TC estimation. However, it is still challenging for automatic TC estimation methods because of the textural variations of different tissue types and the tissue color variations induced by differences in the slide generation process [10,11].

Still, there are lots of methods proposed trying to achieve accurate TC estimation in a fully automatic manner. Peikari et al. [12] utilized the traditional machine learning method to estimate tumor cellularity. They first conducted nuclei segmentation and malignant epithelial figures classification, then performed cellularity estimation based on the malignant images. Likewise, Akbar et al. [14]

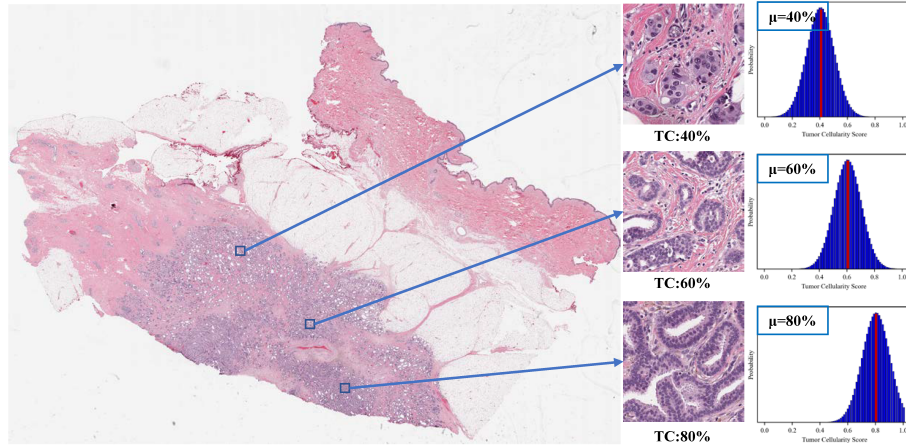


Fig. 1. The illustration of the tumor cellularity (TC) assessment task and the core idea of the proposed ULTRA which transfers the traditional TC regression problem to a label distribution learning [13] problem.

proposed to conduct tumor cellularity assessment by measuring the proportion of malignant cells in the region of interest (ROI). Although the above methods have made some progress on TC estimation, they need nuclei segmentation labels which are expensive to obtain, and the performance is relatively poor. To address the above problems, Rakhlin et al. [15] performed TC estimation with a cellularity score regression method, which skipped the intermediate segmentation and achieved superior results. Similarly, Akbar et al. [16] proposed to regress tumor cellularity with ResNet [17] directly. They trained a series of ResNet architectures to conduct regression tasks, and achieved better results than traditional machine learning methods. Although those techniques achieved

superior performance compared to the segmentation-based methods, they took TC estimation as a simple regression problem and ignored the intrinsic ambiguity of the TC labels caused by subjective assessment or multiple raters, which further restricted the performance improvements.

Inspired by [13,18,19], we proposed an **Uncertainty-aware Label disTRibution leArning (ULTRA)** framework that fully leverages the label ambiguity (uncertainty) for TC estimation. The core idea is illustrated in Fig. 1. The ULTRA first converted the single-value TC labels to discrete label distributions, which effectively models the ambiguity among all possible TC labels. Furthermore, the network learned the TC label distributions by minimizing the Kullback-Leibler (KL) divergence between the predicted and ground-truth TC label distributions, which better supervised the model to leverage the ambiguity of TC labels caused by subjective assessment. Moreover, the ULTRA mimicked the multi-rater fusion process in clinical routines with a multi-branch feature fusion module to further explore the uncertainties of TC labels from multiple raters. The main contributions of our paper are three-fold:

- We are the first to model label ambiguity (uncertainty) of TC labels by transferring the TC score regression to a label distribution learning problem.
- We proposed a multi-branch feature fusion module by mimicking the multi-rater fusion process in clinical routines, which effectively leveraged the label uncertainty and significantly improved the TC estimation performance.
- Our ULTRA outperforms both segmentation-based and regression-based methods on the TC estimation task and achieved state-of-the-art results on the SPIE-AAPM-NCI BreastPathQ dataset.

2 Methods

The ULTRA aims to effectively exploit the uncertainty of the labels in breast tumor cellularity tasks by modeling the label ambiguity with a label distribution rather than a single value. As is illustrated in Fig.2, it mainly consists of three parts: label distribution generation, multi-branch feature fusion, and label distribution learning. The details of each module are as follows:

2.1 Label Distribution Generation

Following [18, 19], we first converted the single-value TC labels to discrete label distributions, which effectively models the ambiguity among all possible TC labels. The TC distribution comprises a group of probability values which represent the description degree of each TC value for the input image. Specifically, to generate label distributions based on the TC scores, we first quantize the TC score ranges $[0, 1]$ into an ordered label set $t \in \{t_1, t_2, t_i, \dots, t_n\}$, where n is the number of discretized labels, $t_i \in [0, 1]$ are possible TC scores. We set $n = 100$

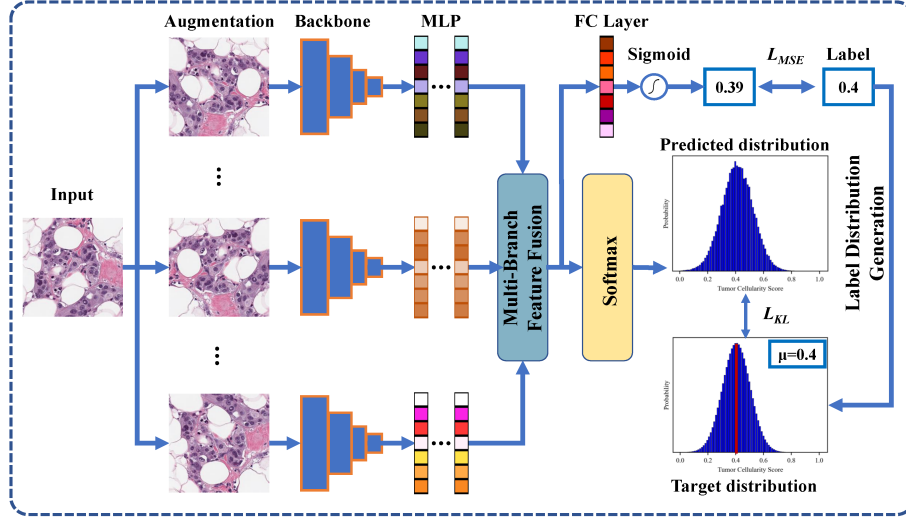


Fig. 2. The overview of the proposed ULTRA. The input image patches are first augmented and fed into the backbone network to extract features. Furthermore, the feature maps are processed by MLPs in different branches and fused with multi-branch feature fusion. Finally, the network is optimized by jointly performing TC distribution learning and score regression.

according to the precision of TC labels. Given a TC value s of a specific image, we then constructed a Gaussian distribution with label set t :

$$G(t_i | s, \sigma) = \frac{1}{\sqrt{2\pi}\sigma} \exp\left(-\frac{(t_i - s)^2}{2\sigma^2}\right) \quad (1)$$

where s is the TC label and also the mean value of the Gaussian distribution. σ is the hyper-parameter that defines the sharpness of the Gaussian distribution and can be also taken as the uncertainty of TC score. We set $\sigma = 0.04$ in our implementation since it achieved better results than other settings. Considering that a label distribution $y_i, i \in \{1, 2, \dots, n\}$ should satisfy two constrains, i.e., $y_i \in [0, 1]$, and $\sum_i y_i = 1$, we finally generate the TC label distribution by normalizing the Gaussian distribution:

$$y_i = \frac{G(t_i | s, \sigma)}{\sum_k G(t_k | s, \sigma)} \quad (2)$$

2.2 Multi-Branch Feature Fusion

To further explore the TC label uncertainties caused by multiple raters, we mimicked the multi-rater fusion process with a Multi-Branch Feature Fusion module (MBFF). The proposed MBFF significantly improved the TC estimation performance by effectively modeling the estimation process of multiple raters and

leveraging the ambiguity among them. Specifically, given an input image I , we designed multiple branches to process it, and each branch represents the annotation process of a single rater. In a specific branch, we first applied augmentation methods to increase the variabilities of the input and further improve the generalization performance of the network; \hat{I}_k denotes the processed image with augmentations at branch k . Then, the augmented image was further processed by a backbone network and an MLP in each branch, which modeled the decision process for a single rater. Finally, each branch generated various rich hierarchical features, which encoded valuable information for the annotation of the input image:

$$f^k = \mathcal{F}_{MLP} \left(\mathcal{F}_{Backbone} \left(\hat{I}_k \right) \right) \quad (3)$$

where \mathcal{F}_{MLP} and $\mathcal{F}_{Backbone}$ represent the MLP and the backbone network. f^k are the feature maps at branch k . We used ResNet34 as the backbone network and three fully connected layers as the MLP in our implementation.

Furthermore, to better exploit the uncertainties among different raters, we introduced MBFF which calculated the weighted average among features from different branches. Finally, we achieved the enhanced feature maps as follows:

$$f_{enhanced} = \frac{1}{N} \sum_{k=1}^N W_k f^k \quad (4)$$

where W_k is the relative importance of different branch, in our implementation, we set $W_k = 1$ in all branches, empirically.

2.3 Label Distribution Learning

The proposed ULTRA transfers the traditional TC regression problem to a label distribution learning problem (LDL), which better supervises the model to leverage the ambiguity of TC labels. Based on the hierarchical features generated from the MBFF, the predicted TC distribution can be achieved by applying a softmax activation function:

$$p_i = \frac{\exp(f_{enhanced}^i)}{\sum_i \exp(f_{enhanced}^i)}, \quad i = 0, 1, 2, \dots, n \quad (5)$$

where $f_{enhanced}^i$ denotes the i th channel of enhanced feature from MBFF. Finally, we minimize the Kullback-Leibler (KL) divergence between the estimated TC distribution p_i and the normalized Gaussian distribution y_i :

$$\mathcal{L}_{KL} = KL \{ \mathbf{p}_i \| \mathbf{y}_i \} = \sum_i p_i \log \frac{p_i}{y_i} \quad (6)$$

Moreover, existing label distribution learning suffers from severe object mismatch problem [20, 21]. Therefore, different from existing methods in [18, 19], which simply supervise the model with the KL divergence loss, we added an extra regression branch with mean square error loss function to mitigate the object

mismatch problem, and finally jointly performed TC distribution learning and TC score regression in a multi-task learning manner:

$$\mathcal{L} = \mathcal{L}_{KL} + \alpha\mathcal{L}_{MSE} \quad (7)$$

where α represents the relative weight to balance the importance of label distribution learning and TC score regression. Specifically, we empirically set $\alpha = 1$ in our experiments. \mathcal{L}_{MSE} denotes the mean square error between predicted TC score and labels.

3 Experiments and Results

3.1 Materials and Evaluation Metrics

To demonstrate the effectiveness of the proposed method, we utilized the public SPIE-AAPM-NCI BreastPathQ³ dataset [22] in our study. The dataset provides 2394 and 185 patches with TC labels ranging from 0% to 100% in the training and validation set, and 1119 patches for testing whose TC labels are unavailable.

Following [15], we adopted intra-class correlation (ICC) [23], Cohen’s kappa (Kappa) [24] and mean square error (MSE) as the evaluation metrics.

3.2 Implementation Details

Our model was trained on the NVIDIA RTX 2080Ti GPU for 150 epochs. In the training phase, we first normalized the input data by subtracting the mean and dividing it by the standard deviation. In addition, we randomly performed different augmentations in MBFF including horizontal, vertical flips, elastic transforms, and etc. Besides, we utilized the Adam optimizer and set the initial learning rate to 1e-4, and the learning rate decayed by multiplying 0.1 every 100 epochs. We set the batch size to 8 in all our experiments empirically. We performed a two-stage training scheme: first stage for backbone training and the second stage for the whole framework training. In the testing phase, the input patches are also randomly augmented to perform multi-branch feature fusion, and then the network predicts the TC distributions for input patches. After obtaining the predicted TC distribution by performing the softmax function, the TC assessment is obtained by selecting the TC value with the largest probability among all possible TC scores. Finally, the predicted TC score is achieved by averaging the predictions from regression and label distribution branches.

3.3 Experimental Results and Discussion

Effectiveness of the MBFF: Table 1 shows the ablation study on the MBFF module. We tested three ULTRA variations with different numbers of branches, $N = \{1, 2, 3\}$. Experimental results demonstrate that the ULTRA with MBFF

Table 1. Ablations of the MBFF, N : number of branches. \uparrow : The larger, the better; \downarrow : The smaller, the better.

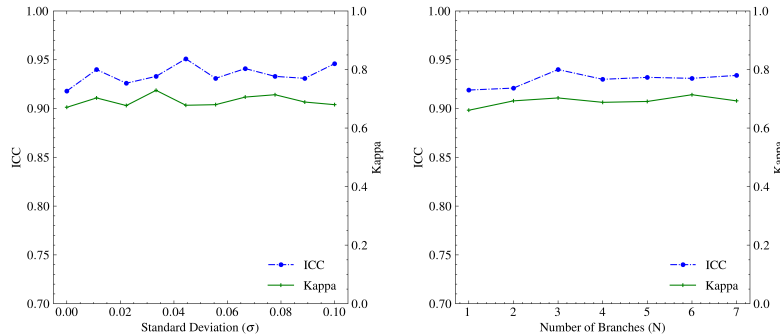
Model	ICC \uparrow	Kappa \uparrow	MSE \downarrow
ULTRA (N=1)	0.919	0.688	0.013
ULTRA (N=2)	0.921	0.693	0.014
ULTRA (N=3)	0.941	0.703	0.011

Table 2. Ablations of the LDL and regression for the ULTRA. \uparrow : The larger, the better; \downarrow : The smaller, the better.

Model	ICC \uparrow	Kappa \uparrow	MSE \downarrow
ULTRA w/o KL	0.918	0.600	0.012
ULTRA w/o MSE	0.926	0.650	0.014
ULTRA	0.941	0.703	0.011

module outperforms its variants without fusion (i.e., $N=1$). This further proves the effectiveness of the MBFF.

Effectiveness of The LDL: Table 2 illustrates the experimental results in different settings. It demonstrates that the ULTRA with only LDL branch outperforms that of regression branch in ICC and Kappa, while slightly inferior in MSE. Moreover, the above two variants are inferior to the normal ULTRA in all metrics. This proves that the LDL effectively leveraged the label uncertainty and improved the TC estimation results. More importantly, the proposed ULTRA further enhanced the performance by combining the LDL and TC regression.



(a) Results on different Standard Deviation of Gaussian distribution (b) Results on different number of branches

Fig. 3. The experimental results on different hyper-parameter settings

Different Hyper-parameter Settings: We performed experiments to investigate the impact of two significant hyper-parameter settings: (1) Different σ for Gaussian distribution. Following [18], we uniformly sampled 10 values for σ in range $[0, 0.1]$. Fig.3(a) illustrates the results for different σ . It shows that σ should be set neither too large nor too small. This is reasonable since σ controls the uncertainty of the TC label, large σ would introduce extra label noise, while small σ would not be enough to represent the ambiguity. (2) Different number

³ <https://breastpathq.grand-challenge.org/>

Table 3. Quantitative results (Mean with 95% confidence intervals) of state-of-the-art methods on BreastPathQ validation set. Bold text denotes the best result for that column. "-" means the authors didn't report that metric.

Methods	Metrics		
	ICC \uparrow	Kappa \uparrow	MSE \downarrow
Baseline	0.901[0.870,0.930]	0.688[0.602,0.774]	0.015[0.011,0.019]
Peikari et al. [12]	0.750[0.710,0.790]	0.380-0.420	-
Akbar et al. [14]	0.830[0.790,0.860]	-	-
Rakhlín et al. [15]	0.883[0.858,0.905]	0.689[0.642,0.734]	0.010[0.009,0.012]
Ours(ULTRA)	0.941[0.920,0.950]	0.703[0.620,0.787]	0.011[0.007,0.014]

of branches. Except for $N = \{1, 2, 3\}$, we tested more settings on the number of branches. Fig.3(b) shows the results for different branches. The experimental results first improve and then decrease, finally tend to stable with the improvement of branches. $N = 3$ achieves the best results.

Comparing with State-of-the-art Methods: We compared the experimental results with some SOTA methods including Peikari et al. [12], Akbar et al. [14], and Rakhlín et al. [15]. We also compared the results of a baseline network that performed direct regression with ResNet34. The proposed ULTRA takes the ResNet34 as the backbone network to ensure a fair comparison. Table 3 shows the experimental results on the BreastPathQ validation set. It demonstrates that the proposed ULTRA outperforms all other state-of-the-art methods on both ICC and Kappa metrics for a large margin and achieved comparable results on the MSE metric. The superior TC estimation results further prove the effectiveness of the proposed method. In addition, we performed t-test between the ULTRA and other SOTA methods, the experimental results prove that the superiority of the ULTRA is statistically significant (p-value<0.001, p-value<0.005, p-value<0.01 for ICC, Kappa and MSE, respectively). Moreover, we also compared the corresponding TC scores generated by each method on WSIs of the BreastPathQ validation set, which is illustrated in Fig.4. It demonstrates that the TC scores generated from the proposed methods are closer to the ground-truth labels than other techniques, proving that the proposed method can effectively assess breast tumor cellularity.

4 Conclusion

In this paper, we proposed ULTRA to address the problem of ignoring label ambiguity for the tumor cellularity assessment task. The proposed ULTRA transformed TC regression to a label distribution learning problem, which significantly exploited the label ambiguity of the TC scores. Moreover, by mimicking the multi-rater fusion process in clinical routines, the framework further leveraged the label uncertainty and improved the TC estimation performance. Experimental results prove that the proposed ULTRA achieved superior performance compared to many state-of-the-art methods.

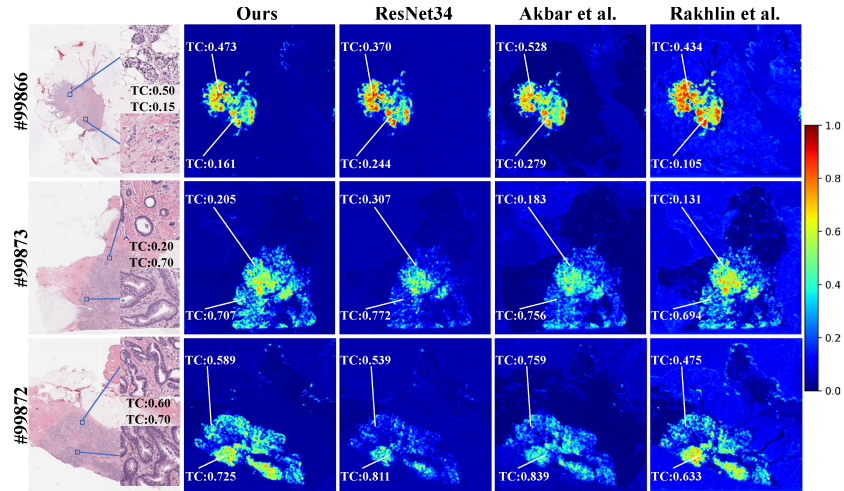


Fig. 4. TC scores generated on WSIs of the BreastPathQ validation set. The blue color denotes healthy tissue (TC=0%) and red denotes malignant (TC = 100%).

Acknowledgments

This work was supported by the National Natural Science Foundation of China under Grant Grant 62001144 and 62001141, and by Science and Technology Innovation Committee of Shenzhen Municipality under Grant JCYJ20210324131800002 and RCBS20210609103820029.

References

1. Key, T.J., Verkasalo, P.K., Banks, E.: Epidemiology of breast cancer. *The lancet oncology* **2**(3) (2001) 133–140
2. Thompson, A., Moulder-Thompson, S.: Neoadjuvant treatment of breast cancer. *Annals of Oncology* **23** (2012) x231–x236
3. Loibl, S., Denkert, C., von Minckwitz, G.: Neoadjuvant treatment of breast cancer—clinical and research perspective. *The Breast* **24** (2015) S73–S77
4. Rubovszky, G., Horváth, Z.: Recent advances in the neoadjuvant treatment of breast cancer. *Journal of Breast Cancer* **20**(2) (2017) 119–131
5. Rajan, R., Poniecka, A., Smith, T.L., Yang, Y., Frye, D., Pusztai, L., Fiterman, D.J., Gal-Gombos, E., Whitman, G., Rouzier, R., et al.: Change in tumor cellularity of breast carcinoma after neoadjuvant chemotherapy as a variable in the pathologic assessment of response. *Cancer: Interdisciplinary International Journal of the American Cancer Society* **100**(7) (2004) 1365–1373
6. Kumar, S., Badhe, B.A., Krishnan, K., Sagili, H.: Study of tumour cellularity in locally advanced breast carcinoma on neo-adjuvant chemotherapy. *Journal of clinical and diagnostic research: JCDR* **8**(4) (2014) FC09
7. Park, C.K., Jung, W.H., Koo, J.S.: Pathologic evaluation of breast cancer after neoadjuvant therapy. *Journal of pathology and translational medicine* **50**(3) (2016) 173

8. Symmans, W.F., Peintinger, F., Hatzis, C., Rajan, R., Kuerer, H., Valero, V., Assad, L., Poniecka, A., Hennessy, B., Green, M., et al.: Measurement of residual breast cancer burden to predict survival after neoadjuvant chemotherapy. *Journal of Clinical Oncology* **25**(28) (2007) 4414–4422
9. Smits, A.J., Kummer, J.A., De Bruin, P.C., Bol, M., Van Den Tweel, J.G., Seldenrijk, K.A., Willems, S.M., Offerhaus, G.J.A., De Weger, R.A., Van Diest, P.J., et al.: The estimation of tumor cell percentage for molecular testing by pathologists is not accurate. *Modern Pathology* **27**(2) (2014) 168–174
10. Madabhushi, A., Lee, G.: Image analysis and machine learning in digital pathology: Challenges and opportunities. *Medical image analysis* **33** (2016) 170–175
11. Tizhoosh, H.R., Pantanowitz, L.: Artificial intelligence and digital pathology: challenges and opportunities. *Journal of pathology informatics* **9** (2018)
12. Peikari, M., Salama, S., Nofech-Mozes, S., Martel, A.L.: Automatic cellularity assessment from post-treated breast surgical specimens. *Cytometry Part A* **91**(11) (2017) 1078–1087
13. Geng, X.: Label distribution learning. *IEEE Transactions on Knowledge and Data Engineering* **28**(7) (2016) 1734–1748
14. Akbar, S., Peikari, M., Salama, S., Panah, A.Y., Nofech-Mozes, S., Martel, A.L.: Automated and manual quantification of tumour cellularity in digital slides for tumour burden assessment. *Scientific reports* **9**(1) (2019) 1–9
15. Rakhlin, A., Tiulpin, A., Shvets, A.A., Kalinin, A.A., Iglovikov, V.I., Nikolenko, S.: Breast tumor cellularity assessment using deep neural networks. In: *Proceedings of the IEEE/CVF International Conference on Computer Vision Workshops*. (2019) 0–0
16. Akbar, S., Peikari, M., Salama, S., Nofech-Mozes, S., Martel, A.L.: Determining tumor cellularity in digital slides using resnet. In: *Medical Imaging 2018: Digital Pathology*. Volume 10581., International Society for Optics and Photonics (2018) 105810U
17. He, K., Zhang, X., Ren, S., Sun, J.: Deep residual learning for image recognition. In: *Proceedings of the IEEE conference on computer vision and pattern recognition*. (2016) 770–778
18. Gao, B.B., Xing, C., Xie, C.W., Wu, J., Geng, X.: Deep label distribution learning with label ambiguity. *IEEE Transactions on Image Processing* **26**(6) (2017) 2825–2838
19. Tang, Y., Ni, Z., Zhou, J., Zhang, D., Lu, J., Wu, Y., Zhou, J.: Uncertainty-aware score distribution learning for action quality assessment. In: *Proceedings of the IEEE/CVF Conference on Computer Vision and Pattern Recognition*. (2020) 9839–9848
20. Wang, J., Geng, X.: Label distribution learning machine. In: *International Conference on Machine Learning*, PMLR (2021) 10749–10759
21. Wang, J., Geng, X., Xue, H.: Re-weighting large margin label distribution learning for classification. *IEEE Transactions on Pattern Analysis and Machine Intelligence* (2021)
22. Petrick, N., Akbar, S., Cha, K.H., Nofech-Mozes, S., Sahiner, B., Gavrielides, M.A., Kalpathy-Cramer, J., Drukker, K., Martel, A.L., et al.: Spie-aapm-nci breastpathq challenge: an image analysis challenge for quantitative tumor cellularity assessment in breast cancer histology images following neoadjuvant treatment. *Journal of Medical Imaging* **8**(3) (2021) 034501
23. Shrout, P.E., Fleiss, J.L.: Intraclass correlations: uses in assessing rater reliability. *Psychological bulletin* **86**(2) (1979) 420

24. McHugh, M.L.: Interrater reliability: the kappa statistic. *Biochemia medica* **22**(3) (2012) 276–282